EURASIP Journal on Applied Signal Processing 2003:5, 405–412

Dynamic MR-Imaging with Radial Scanning, a Post-Acquisition Keyhole Approach

Ralf Lethmate

Laboratoire de Résonance Magnétique Nucléaire, CNRS UMR 5012, Université Claude Bernard Lyon I, CPE, France
Email: rle@soft-imaging.de

Frank T. A. W. Wajer

Department of Applied Physics, Delft University of Technology, P.O. Box 5046, 2600 GA, Delft, The Netherlands
Email: frank.wajer@nl.thalesgroup.com

Yannick Crémillieux

Laboratoire de Résonance Magnétique Nucléaire, CNRS UMR 5012, Université Claude Bernard Lyon I, CPE, France
Email: yannick.cremillieux@univ-lyon1.fr

Dirk van Ormondt

Department of Applied Physics, Delft University of Technology, P.O. Box 5046, 2600 GA, Delft, The Netherlands
Email: ormo@si.tn.tudelft.nl

Danielle Graveron-Demilly

Laboratoire de Résonance Magnétique Nucléaire, CNRS UMR 5012, Université Claude Bernard Lyon I, CPE, France
Email: danielle.graveron@univ-lyon1.fr

Received 15 February 2002

A new method for 2D/3D dynamic MR-imaging with radial scanning is proposed. It exploits the inherent strong oversampling in the centre of k-space, which holds crucial temporal information of the contrast evolution. It is based on (1) a rearrangement of (novel 3D) *isotropic* distributions of trajectories during the scan according to the desired time resolution and (2) a post-acquisition *keyhole* approach. The 2D/3D dynamic images are reconstructed using 2D/3D-gridding and 2D/3D-IFFT. The scan time is not increased with respect to a *conventional* 2D/3D radial scan of the same image resolution, in addition one benefits from the dynamic information. An application to in vivo ventilation of rat lungs using hyperpolarized helium is demonstrated.

Keywords and phrases: 2D/3D dynamic MRI, 3D isotropic radial sampling, keyhole, scan time reduction, image reconstruction, gridding.

1. INTRODUCTION

Dynamic magnetic resonance imaging (MRI) is a challenging topic that opens a vast field in medical diagnosis such as contrast-enhanced MR angiography, hyperpolarized gas imaging, perfusion, interventional imaging, and functional brain imaging. Dynamic (time-resolved) images have to be acquired within a reasonable time scale and with reasonable spatial and temporal resolution. But, 3D-MRI techniques are in general very time-consuming and inadequate for recording dynamic features.

In MRI, signals are measured in Fourier space, the so-called k-space [1, 2]. One commonly used approach for improving the temporal resolution of dynamic MR imaging is the sliding window technique [3], which updates the most recently acquired region of k-space before each image reconstruction. Other techniques exist such as TRICKS [4] and Glimpse [5] which update the inner part of k-space more frequently than the outer part or have more optimum phase-encoding strategies [6]. For non-Cartesian sampling, undersampled projection reconstruction [7], the recent VIPR method [8, 9] and variable density spirals [10, 11] have also been proposed.

Our method for dynamic imaging exploits the inherent strong oversampling of radial scanning in the centre of k-space, which holds crucial temporal information of the contrast evolution. The essence of the method is based on updating the centre of k-space in the same vein as with conventional Cartesian keyhole acquisitions [12]. The difference is that our method is a "*post*-acquisition keyhole" technique needing no additional data. To achieve an n-fold increase of the temporal resolution, the temporal orders of the trajectories are rearranged during the scan such that *n isotropic* subdistributions are obtained in n time slots. The radial sampling distribution itself and the number of scanned trajectories do not change with respect to a conventional 3D radial scan of the same resolution, in addition one benefits from the dynamic information.

In MRI, the commonly used 3D radial sampling distributions pertain to the so-called projection reconstruction (PR) distributions [13, 14]. Unlike 2D-PR sampling distributions [15, 16], 3D-PR sampling distributions are not isotropic: the polar regions of k-space are too densely sampled which is disadvantageous for dynamic imaging. So, for 3D imaging, the method needs using of *isotropic* radial sampling distributions, such as the linear and trigonometric equidistributions or hexagonal equidistributions that we recently proposed in MRI [17, 18, 19, 20]. These equidistributions guarantee minimal scan time and prevent undersampling artifacts.

Reconstructions of the n 2D/3D dynamic images are performed via resampling onto a Cartesian grid using a 2D/3D-gridding algorithm [21, 22, 23, 24] followed by 2D/3D-IFFT.

Results are shown both for 2D and 3D imaging using real-world data. An application to ventilation of rat lungs using hyperpolarized helium (^{3}He) is demonstrated for 2D.

2. METHOD

2.1. *Isotropic radial sampling equidistributions*

In radial scanning, k-space is sampled along trajectories which are straight lines going either from the centre to the edge or from one edge to the opposite edge through the centre. Along each trajectory, sampling is uniform. The commonly used radial 2D/3D sampling distributions are PR distributions [13, 14, 15, 16]. Each radial trajectory is such that the samples reside on radials as well as on concentric circles/spheres, see Figure 1. The directions of the trajectories are equally distributed between 0 and 2π for 2D-PR sampling distributions. In 3D-PR, the sampling pattern resembles the mesh grid of the model globe, see Figure 2. Unlike 2D-PR sampling distributions, 3D-PR sampling distributions are not isotropic: the polar regions of k-space are extensively oversampled, see Figure 1. This is disadvantageous in terms of scan time and image resolution, mainly for dynamic imaging.

We recently proposed novel more isotropic radial sampling distributions for 3D radial static MRI scans [17, 18, 19, 20], the linear equidistribution (LE) and trigonometric equidistribution (TE) taken from geomathematical applications [25] and the hexagonal equidistribution (Hex) [26] that we consider to be a near optimal spherical equidistribution. To the best of our knowledge, these equidistributions are applied to MRI by our group for the first time. Figure 2 shows the angular maps of 3D-PR, LE, and Hex distributions in spherical coordinates. For 3D-PR, the map is a Cartesian grid; again, one can see that the poles are excessively oversampled.

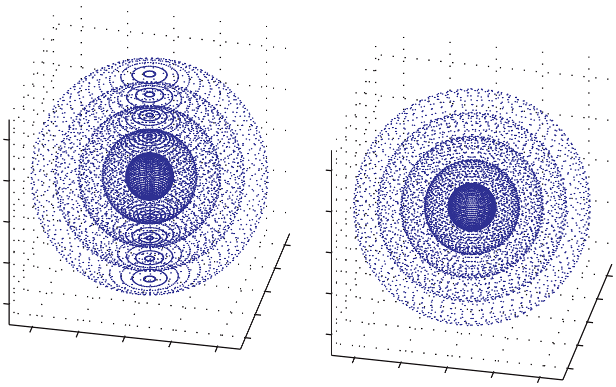

FIGURE 1: 3D-PR (left) and linear equidistribution (LE). Only the first five shells are shown.

We have shown that the LE/TE and Hex sampling equidistributions both yield a scan time reduction of more than 30% with respect to the 3D-PR [17, 20] which is crucial for dynamic imaging. They are the 3D sampling distributions of choice when using the proposed 3D radial dynamic keyhole method.

2.2. *Post-acquisition keyhole technique*

k-space can be considered to be spanned by the four vectors $\vec{k}_x$, $\vec{k}_y$, $\vec{k}_z$, and $\vec{t}$. The method aims at reconstructing dynamic images $I(x, y, z, t)$, where x, y, z stand for the spatial coordinates and t for the time, with the best temporal and spatial resolution. This can be done by taking the advantage of the oversampled central k-space area of radial scans which contains much of the temporal information needed for dynamic studies.

In 2D, 2D-PR represents the perfect sampling equidistribution. Such a distribution with a clockwise readout of the trajectories is shown in a 3D-plot in Figure 3. This figure visualizes clearly that not only the spatial information of k-space is sampled but also the temporal information. The trajectories can be scanned in any arbitrary temporal order, as long as a sufficient number of trajectories cover k-space *uniformly*. This has to be respected in order to prevent image artifacts through angular undersampling.

The gist of the method is based on rearranging the temporal order of the trajectories during the scan such that n isotropic subdistributions S_i are obtained in n time slots i. The k-space centres (or k-space cores S_i^{core}) of the subdistributions must be fully sampled, see Figure 4. For 3D, the n sampling subdistributions of the LE/TE or Hex equidistributions S are obtained by associating every nth trajectory to a same subdistribution S_i, reading the colatitude and azimuth angular map of the distribution from north to south and from west to east, see Figure 2. Outside each core (mantle), one simply uses the samples on all trajectories acquired

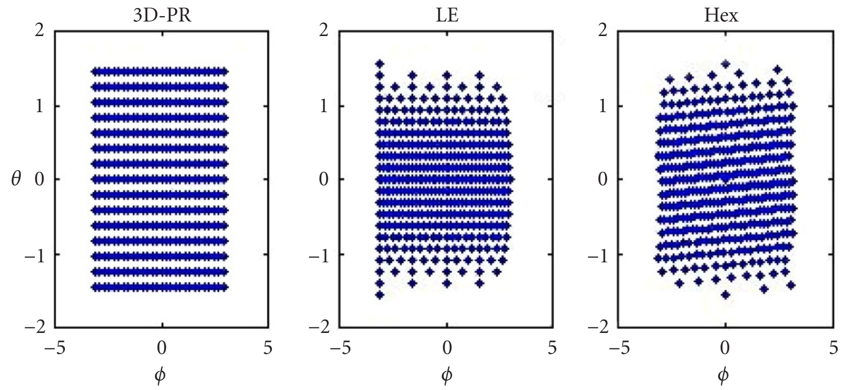

FIGURE 2: Angular maps of the different sampling distributions using spherical coordinates (units in radians).

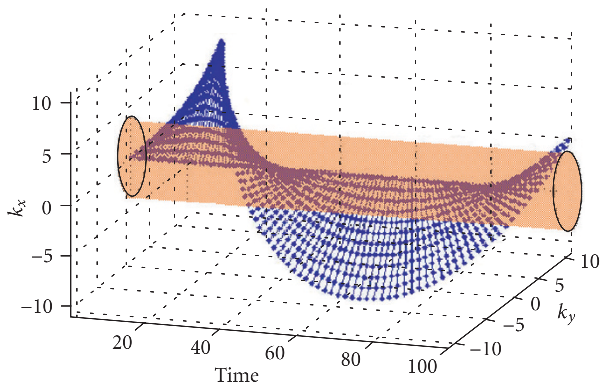

FIGURE 3: 2D-PR sampling distribution with a clockwise readout of the trajectories and additional temporal information. The shaded area is no longer oversampled with respect to space and time.

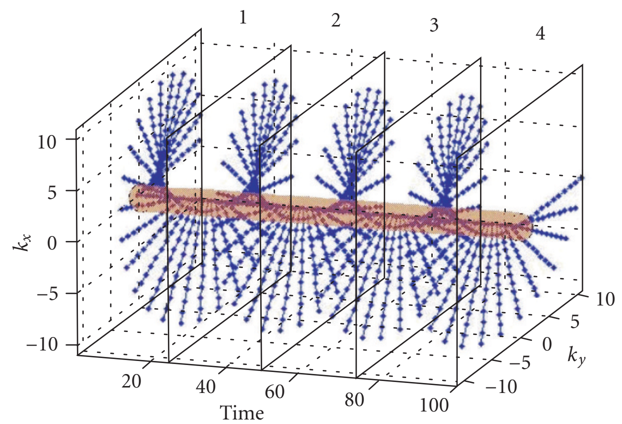

FIGURE 4: The same 2D-PR sampling distribution as in Figure 3 with reordered trajectories, see also Figure 5. Nyquist's sampling criterion is now satisfied in short "k-space time slots" $[k_x, k_y, \Delta t]$ from k_0 till a radius k_{core} within one subdistribution.

during the entire measurement. The cores S_i^{core} of the n sampling subdistributions S_i contain most of the contrast information, and replace S^{core} of the complete equidistribution S, leading to n sufficiently sampled "keyholed" k-spaces S_i, such that $S_i = (S \setminus S^{\text{core}}) \cup S_i^{\text{core}}$, see Figure 5. For 3D, the method is sketched in Figure 6. The cores S_i^{core} can hence be considered to update S at n different time slots t_i. Outside the cores, the dynamic effects are averaged. The latter is done in the same vein as with conventional Cartesian "keyholing" [12]. The difference with the latter is that our method is a post-acquisition keyhole technique needing no additional data. With Cartesian keyhole imaging, a complete reference k-space must be acquired first. Then, for all subsequent images, the central trajectories are measured again. Before image reconstruction, the central trajectories of the dynamic k-spaces are combined with the outer trajectories of the whole data set.

In our post-acquisition keyhole technique the number of subdistributions defines the temporal resolution Δt, which is $\Delta t = N_r\,\text{TR}/n$, N_r being the total number of scanned trajectories and TR the time between the scan of two successive trajectories (the repetition time in MR jargon). The temporal resolution is increased by a factor of n with respect to the conventional image.

The choice of the core/keyhole radius is important and is sensitive to the chosen number of trajectories N_r. Provided that sampling starts at the centre of k-space, Nyquist's criterion is satisfied when $N_r = \pi N$ in 2D and when $N_r = \pi N^2$ for perfect 3D equidistributions. This means that in each time slot Nyquist's criterion is satisfied only in a range from $\vec{k} = \vec{0}$ up to $|\vec{k}_{\text{core}}|$ with

$$\begin{aligned} |\vec{k}_{\text{core}}| &= \frac{N_r}{2n\pi} \quad \text{for 2D,} \\ |\vec{k}_{\text{core}}| &= \sqrt{\frac{N_r}{4n\pi}} \quad \text{for 3D.} \end{aligned} \tag{1}$$

The dynamic effects are averaged beyond $|\vec{k}_{\text{core}}|$ because we use the information of the entire scan. But the crucial contribution of this region to the desired *spatial* resolution is

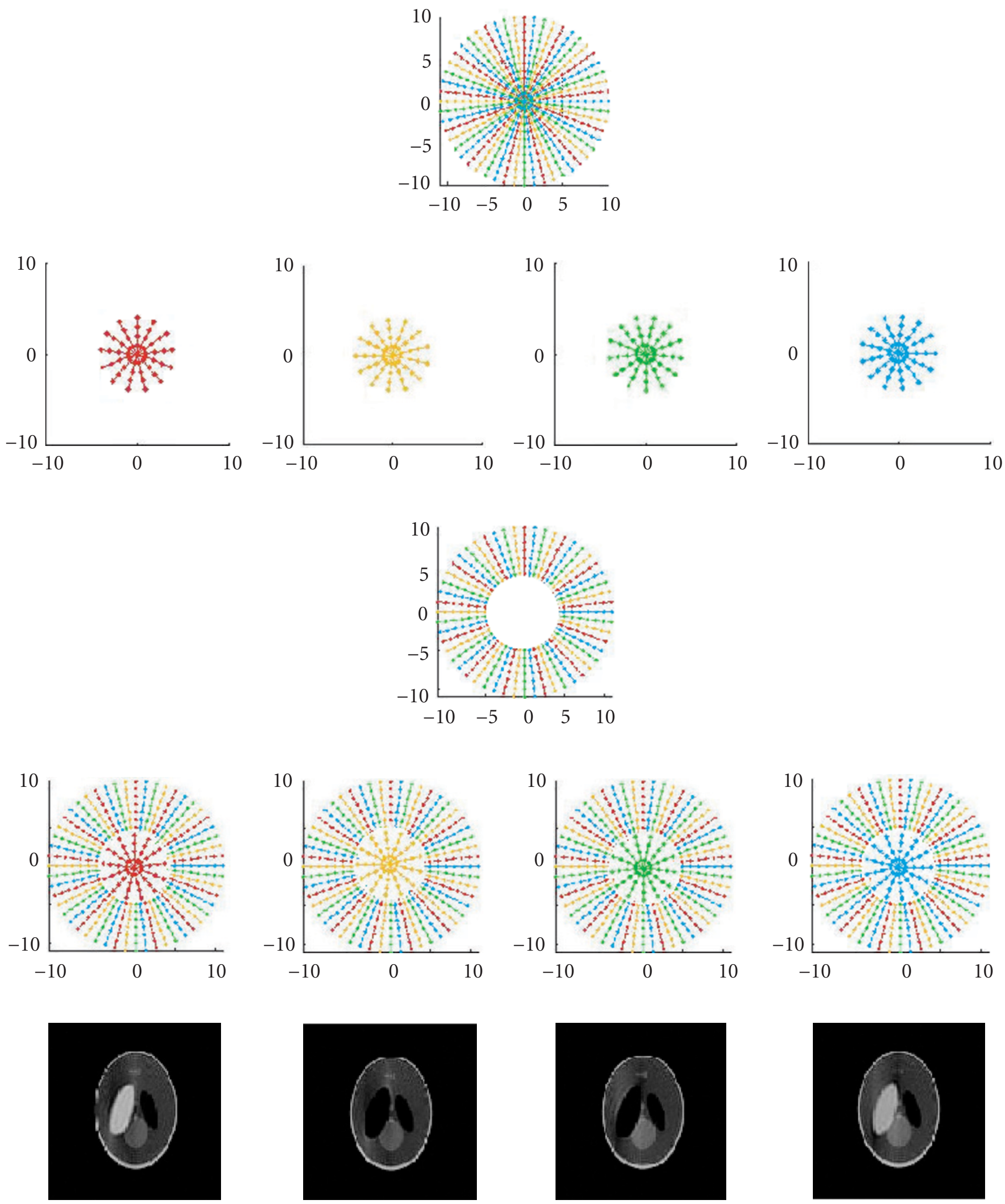

Figure 5: Scheme of our post-acquisition keyhole technique. Radial trajectories associated to the same time slot/subdistribution are labeled with the same grey level. The cores of the subdistributions (second row) containing the temporal information are patched into the centre of the complete sampling distribution (fourth row). In this example, the time resolution is increased by a factor of four. Bottom: 2D images of a dynamic Shepp Logan simulation to illustrate the potential of the method.

not affected. Recapitulating, we achieve an n-fold increase of *temporal* resolution at *low* spatial resolution. The trade-off is adequate in most cases.

As an example, for a 2D reconstruction size $N = 128$, about 400 radials are needed to satisfy Nyquist's criterion at the edge of k-space. In order to achieve a 10-fold increase of time resolution, we divide the available measurement time into 10 time slots. To each time slot, we allot $400/10 = 40$ radials whose directions are equally distributed between 0 and 2π. The Nyquist's criterion is satisfied from $\vec{k} = \vec{0}$ up to $|\vec{k}_{\text{core}}| = 7$. The keyhole radius should not therefore be chosen greater to prevent artifacts through angular undersampling.

If we compare our post-acquisition keyhole technique with the commonly used sliding window technique [3] which updates the most recently acquired region of k-space before each image reconstruction, the proposed method leads to images with a slightly lower signal-to-noise ratio (SNR) but prevents inconsistencies in k-space. Moreover, it does not need the acquisition of a full k-space before starting the dynamic study which constitutes a considerable scan time reduction mainly for 3D dynamic imaging.

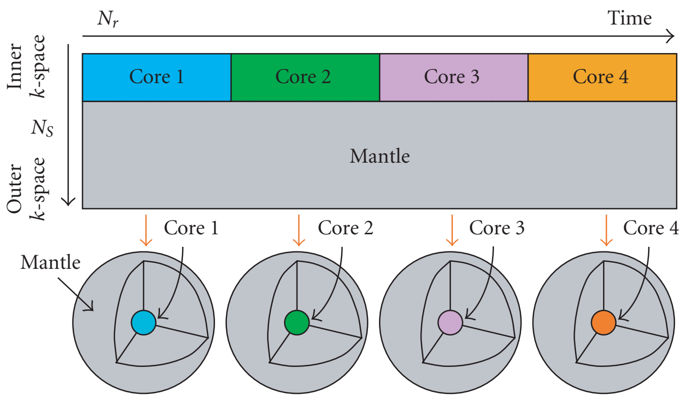

FIGURE 6: Schematic representation of the proposed post-acquisition spherical keyhole method. The scheme shows the insertion of the cores of the $n = 4$ subdistributions S_i into the unchanged outer k-space mantle ($S \setminus S^{\text{core}}$) of the 3D radial sampling distribution S as a function of time.

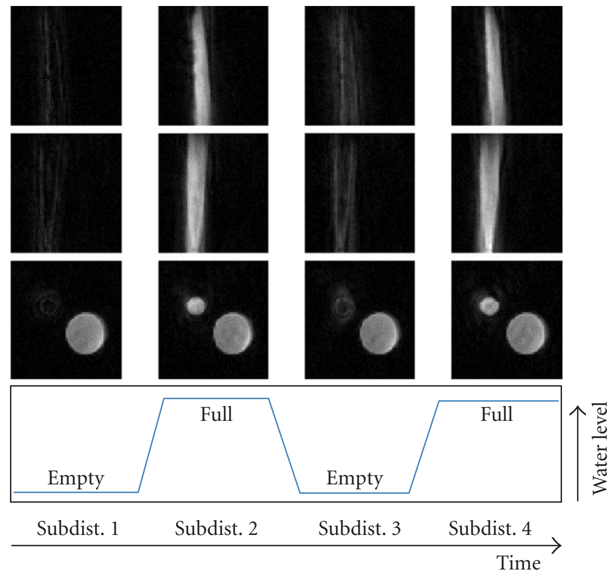

FIGURE 7: Real-world dynamic scan of a bottle filled with water and containing a plastic tube which was alternately filled with water and emptied during the scan, according to the shown paradigm. The LE sampling distribution with $\gamma = 100$ was used which corresponds to the acquisition of 10002 trajectories. The grid size is 128.

2.3. Image reconstruction

Reconstruction of the n 2D/3D images is performed via resampling onto a Cartesian grid using a 2D/3D-gridding algorithm [21, 22, 23, 24, 27] followed by 2D/3D-IFFT. Our gridding algorithm allows high precision image reconstructions from *any* nonuniform sampling distribution. The interpolation is accomplished by convolving the samples with a Kaiser-Bessel kernel [24]. The discretized image $I_{\text{d,g}}$ was computed using the following equation representing the commonly used gridding algorithm:

$$I_{\text{d,g}}(\vec{r}) = \frac{1}{c(\vec{r})} \sum_{l} \left(\sum_{m} [s(k_m)\Delta k_m] C\left(\vec{k}_l - \vec{k}_m\right) \right) e^{2\pi i \vec{k}_l \vec{r}}, \quad (2)$$

where s represents the signal, k_m the nonuniform (radial) samples, k_l the regridded Cartesian samples, and r the spatial coordinate. The terms $C(k)$ and $c(r)$ are the convolution/multiplication window in k-space and image space, respectively. The inner summation is the discrete convolution of the convolution window with the nonuniformly sampled signal. The quantities Δk_m correspond to the inverse of the sampling density. They are to be estimated by a separate procedure, referred to as sampling density compensation. We used the very recent point spread function approach (PSF) [28, 29]. The outer summation is the subsequent IFFT. Finally, the division by $c(r)$ corrects the distorsion induced by the shape of this window in the field of view. For more details about the gridding algorithm, we refer to [24, 27, 30, 31, 32].

Computation of the sampling density compensation is not a trivial matter. We used our own implementation of the point spread function approach. The areas/volumes Δk_m assigned to sample positions are considered as free parameters or weights to be set such that the Fourier transform of the sampling distribution function times the weights approaches a delta function at the centre of image space. The main advantage of this flexible method is that it is adapted to any sampling distribution and consequently to the "keyholed" subdistributions S_i, mainly for 3D image reconstruction. Nevertheless it does not compensate for artifacts due to undersampling.

The temporal spreading of k-space samples does not influence the gridding procedure. As said above, the convolution of the sample points is done with a Kaiser-Bessel window of width L. Any oversampled area within the Kaiser-Bessel window will enhance the SNR but not the resolution. A 3D image with reconstruction size $N = 128$ would theoretically necessitate about 51472 radials to satisfy Nyquist's criterion. With a typical window width of $L = 3$, this means that within the volume around k-space origin there are about 2×51472 samples where 27 would be sufficient for correct image reconstruction. The method reallocates redundant samples of the complete k-space distribution S to the dynamic k-space sampling distributions S_i and their associated dynamic images.

3. RESULTS

To test our dynamic keyhole method, we first performed a 3D experiment on a "phantom." Then, we applied it to ventilation studies of rat lungs using hyperpolarized helium 3.

3.1. 3D dynamic scan of a phantom

A real-world 3D dynamic scan was performed on a horizontal 2T Oxford Instrument magnet, with a 17-cm bore diameter. The MRI sequence was driven by a Magnetic Resonance Research Systems (MRRS, Guilford, Surrey, UK) console. The scanned object (phantom in MR jargon) consisted

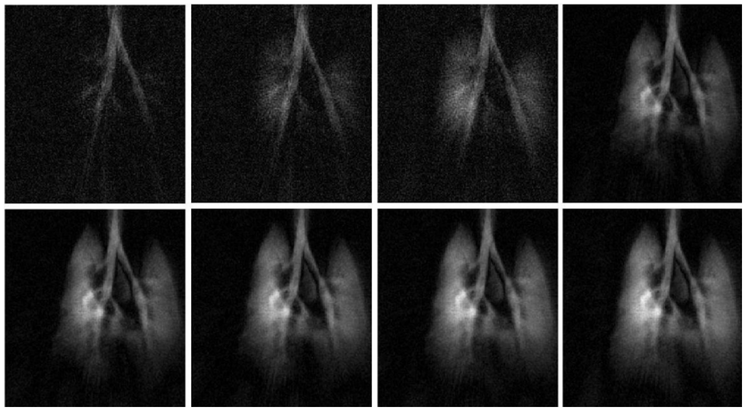

Figure 8: ^{3}He dynamic images of rat lungs obtained with our keyhole method. The images were obtained every 300 milliseconds; only the odd-numbered images are shown. The grid size is 256.

of a bottle, filled with water and a plastic tube. The latter was alternately filled with water and emptied during the scan, according to the paradigm of Figure 7. The LE sampling distribution with $\gamma = 100$ was used. This corresponds to an acquisition of 10002 trajectories and a scan time of 2.5 min. The three rows in Figure 7 show coronal, sagittal, and transverse views of the scanned object. The intensity changes in the tube are clearly visible. The halo around the tube in the dynamic images of the third column is due to the plastic tube itself and not due to the water.

3.2. Application to in vivo dynamic hyperpolarized gas imaging

We applied our post-acquisition keyhole method for dynamic imaging to ventilation of rat lungs using hyperpolarized helium (^{3}He) which is a recent and powerful technique to study lung diseases [33, 34, 35, 36]. The ^{3}He was polarized using a spin-exchange polarizer developed in the Lyon laboratory. Male Sprague-Dawley rats were anaesthetized by intraperitoneal sodium pentobarbital injection, and a catheter was inserted in the trachea connected to a syringe containing 5 ml of ^{3}He. The polarized ^{3}He was delivered to the animal with a controlled rate of 0.5 mL/s.

The experiments were performed on the same horizontal 2T Oxford Instrument magnet, with 17-cm bore diameter. The MRI sequence was driven by an MRRS console. A 6-cm-diameter coil tunable to both ^{1}H and ^{3}He was used. No slice selection was performed and our dynamic 2D-keyhole sequence was used. The parameters for the sequence were TR = 15 ms, sampling interval = 40 μs, flip angle = 10°, and field of view = 80 mm. Two hundred radial trajectories with 128 samples on each were acquired per scan leading to an acquisition time of 3 seconds. Full scans were performed continuously. Each scan was split in 10 dynamic k-spaces such that the temporal resolution is 300 milliseconds per dynamic image. The temporal resolution was increased by a factor of 10. The keyhole radius was 7 samples which was a good trade-off and the dynamic images were reconstructed as described in Section 2.2 using gridding with the PSF sampling density compensation approach. Figure 8 shows our first radial keyhole images. For space reasons, only the odd-numbered images of the dynamic series are displayed. The arrival of polarized ^{3}He in the lungs of the rat is clearly visible.

4. CONCLUSION

We devised a powerful method for dynamic MR-imaging with radial scanning. It exploits the inherent strong oversampling of radial scanning in the centre of k-space, which holds crucial temporal information of the contrast evolution. It is based on

(1) rearranging the temporal order of radial distributions of the trajectories during the scan according to the desired temporal resolution,
(2) construction of n dynamic 3D k-spaces using a post-acquisition keyhole technique based on novel *isotropic* radial sampling equidistributions which guarantee minimal scan time,
(3) reconstruction of n 2D/3D images using 2D/3D-gridding and 2D/3D-IFFT and a PSF approach sampling density compensation.

The temporal resolution is increased by a factor of n. Moreover, the dynamic information of time consuming 3D radial scans can be exploited using the proposed post-acquisition keyhole technique. Contrary to conventional Cartesian keyhole techniques, the full k-space is only acquired once, which constitutes a considerable scan reduction. As shown, the acquisition time is not increased with respect to a *conventional* 2D/3D radial scan of the same spatial resolution, and moreover, one benefits from the extra dynamic information. In addition, the use of the proposed linear/trigonometric and hexagonal sampling equidistributions yields a scan time reduction of more than 30% with respect to 3D-PR which is crucial for dynamic imaging. They are the 3D sampling distributions of choice when using the proposed 3D dynamic keyhole method.

Our method proved already successful for 2D in vivo lung-ventilation imaging using hyperpolarized gas. Other possible applications are contrast-enhanced MR angiography, perfusion, interventional imaging, cancer detection using contrast agents, and functional brain imaging.

ACKNOWLEDGMENTS

This work is supported by the EU Programme TMR, Networks, ERB-FMRX-CT97-0160, and the Dutch Technology Foundation STW, DTN44-3509. The authors thank professor J. P. Antoine for pointing out the applications of equidistributions in geomathematics, V. Stupar for polarizing ^{3}He, and D. Dupuich who set up the ^{3}He experiment.

REFERENCES

[1] M. T. Vlaardingerbroek and J. A. den Boer, *Magnetic Resonance Imaging: Theory and Practice*, Springer-Verlag, Berlin, Germany, 2nd edition, 1999.

[2] E. M. Haacke, R. W. Brown, M. R. Thompson, and R. Venkatesan, *Magnetic Resonance Imaging: Physical Principles and Sequence Design*, Wiley-Liss, New York, NY, USA, 1999.

[3] S. J. Riederer, T. Tasciyan, F. Farzaneh, J. N. Lee, R. C. Wright, and R. J. Herfkens, "MR fluoroscopy: technical feasibility," *Magnetic Resonance in Medicine*, vol. 8, pp. 1–15, 1988.

[4] F. R. Korosec, R. Frayne, T. M. Grist, and C. A. Mistretta, "Time-resolved contrast-enhanced 3D MR angiography," *Magnetic Resonance in Medicine*, vol. 36, no. 3, pp. 345–351, 1996.

[5] R. F. Busse, D. G. Kruger, J. P. Debbins, S. B. Fain, and S. J. Riederer, "A flexible view ordering technique for high-quality real-time 2DFT MR fluoroscopy," *Magnetic Resonance in Medicine*, vol. 42, pp. 69–81, 1999.

[6] A. H. Wilman, S. J. Riederer, B. F. King, J. P. Debbins, P. J. Rossman, and R. L. Ehman, "Fluoroscopically triggered contrast-enhanced three dimensional MR angiography with elliptical centric view order: application to the renal arteries," *Radiology*, vol. 205, pp. 137–146, 1997.

[7] D. C. Peters, F. R. Korosec, T. M. Grist, et al., "Undersampled projection reconstruction applied to MR angiography," *Magnetic Resonance in Medicine*, vol. 43, no. 1, pp. 91–101, 2000.

[8] W. F. Block, A. V. Barger, and C. A. Mistretta, "Vastly undersampled isotropic projection imaging," in *Proc. International Society for Magnetic Resonance in Medicine*, vol. 8, p. 161, Denver, Colo, USA, 2000.

[9] W. F. Block, T. Hany, and A. V. Barger, "Time resolved MRA using undersampled 3D projection reconstruction (VIPR)," in *Proc. International Society for Magnetic Resonance in Medicine*, p. 304, Glasgow, Scotland, UK, 2001.

[10] D. M. Spielman, J. M. Pauly, and C. H. Meyer, "Magnetic resonance fluoroscopy using spirals with variable sampling densities," *Magnetic Resonance in Medicine*, vol. 34, pp. 388–394, 1995.

[11] K. F. King, "Spiral scanning with anisotropic field of view," *Magnetic Resonance in Medicine*, vol. 39, pp. 448–456, 1998.

[12] Philips Medical Systems, Best, The Netherlands, *Basic Principles of MR Imaging*, 1995.

[13] C. M. Lai, "True three-dimensional nuclear magnetic resonance imaging by Fourier reconstruction zeugmatrography," *Journal of Applied Physics*, vol. 52, pp. 1141–1145, 1981.

[14] C. M. Lai and P. C. Lauterbur, "True three-dimensional image reconstruction by nuclear magnetic resonance zeugmatography," *Physics in medicine and biology*, vol. 26, pp. 851–856, 1981.

[15] P. C. Lauterbur, "Image formation by induced local interactions: examples employing nuclear magnetic resonance," *Nature*, vol. 242, pp. 190–191, 1973.

[16] P. C. Lauterbur and C. M. Lai, "Zeugmatography by reconstruction from projections," *IEEE Trans. Nucl. Sci.*, vol. 27, pp. 1227, 1980.

[17] R. Lethmate, J. A. C. van Osch, F. Lamberton, F. T. A. W. Wajer, D. van Ormondt, and D. Graveron-Demilly, "MR image reconstruction from 3D radial sampling distributions. A comparison," in *ProRISC, IEEE Benelux*, vol. 1, pp. 381–387, Veldhoven, The Netherlands, November 2000.

[18] R. Lethmate, J. A. C. van Osch, F. T. A. W. Wajer, D. van Ormondt, and D. Graveron-Demilly, "MR image reconstruction from novel 3D radial sampling distributions," in *Proc. International Society for Magnetic Resonance in Medicine, 9th Scientific and Exhibition, European Society for Magnetic Resonance in Medicine and Biology, 18th Annual Meeting and Exhibition*, p. 781, Glasgow, Scotland, UK, April 2001.

[19] R. Lethmate, J. A. C. van Osch, F. T. A. W. Wajer, D. van Ormondt, and D. Graveron-Demilly, "3D rapid radial dynamic MR-imaging," in *ProRISC, IEEE Benelux*, pp. 489–495, Veldhoven, The Netherlands, November 2001.

[20] R. Lethmate, *Novel radial scan strategies and image reconstruction in MRI*, Ph.D. thesis, Université Claude Bernard, Lyon, France, 2001.

[21] J. I. Jackson, C. H. Meyer, D. G. Nishimura, and A. Macovski, "Selection of a convolution function for Fourier inversion using gridding," *IEEE Trans. on Medical Imaging*, vol. 10, pp. 473–478, 1991.

[22] J. D. O'Sullivan, "A fast sinc function gridding algorithm for Fourier inversion in computer tomography," *IEEE Trans. on Medical Imaging*, vol. 4, no. 4, pp. 200–207, 1985.

[23] H. Schomberg and J. Timmer, "The gridding method for image reconstruction by Fourier transformation," *IEEE Trans. on Medical Imaging*, vol. 14, no. 3, pp. 596–607, 1995.

[24] F. T. A. W. Wajer, R. Lethmate, J. A. C. van Osch, D. Graveron-Demilly, M. Fuderer, and D. van Ormondt, "Interpolation from arbitrary to Cartesian sample positions: gridding," in *ProRISC, IEEE Benelux*, pp. 571–577, Veldhoven, The Netherlands, November 2000.

[25] W. Freeden, T. Gervens, and M. Schreiner, *Constructive Approximation on the Sphere*, Clarendon Press, Oxford, 1998.

[26] E. B. Saff and A. B. J. Kuijlaars, "Distributing many points on a sphere," *Mathematical Intelligencer*, vol. 19, no. 1, pp. 5–11, 1997.

[27] F. T. A. W. Wajer, R. Lethmate, J. A. C. van Osch, D. Graveron-Demilly, and D. van Ormondt, "Simple formula for the accuracy of gridding," in *Proc., International Society for Magnetic Resonance in Medicine, 9th Scientific and Exhibition, European Society for Magnetic Resonance in Medicine and Biology, 18th Annual Meeting and Exhibition*, p. 776, Glasgow, Scotland, UK, April 2001.

[28] J. G. Pipe and P. Menon, "Sampling density compensation in MRI: Rationale and an iterative numerical solution," *Magnetic Resonance in Medicine*, vol. 41, pp. 179–186, 1999.

[29] J. G. Pipe, "Reconstructing MR images from undersampled data: Data-weighting considerations," *Magnetic Resonance in Medicine*, vol. 43, pp. 867–875, 2000.

[30] F. T. A. W. Wajer, G. H. L. A. Stijman, M. Bourgeois, D. Graveron-Demilly, and D. van Ormondt, *Sampling Theory and Practice*, Plenum, New York, NY, USA, 2001.

[31] F. T. A. W. Wajer, D. van Ormondt, M. Bourgeois, and D. Graveron-Demilly, "Non uniform sampling in magnetic resonance imaging," in *Proc. IEEE Int. Conf. Acoustics, Speech, Signal Processing*, pp. 3846–3849, Istanbul, Turkey, June 2000.

[32] F. T. A. W. Wajer, *Non-Cartesian MRI scan time reduction through sparse sampling*, Ph.D. thesis, Delft University of Technology, Delft, The Netherlands, 2001.

[33] H.-U. Kauczor, D. Hofmann, K.-F. Kreitner, et al., "Normal and abnormal pulmonary ventilation: visualization at hyperpolarized He-3 MR imaging," *Radiology*, vol. 201, pp. 564–568, 1996.

[34] E. E. de Lange, J. P. Mugler, J. R. Brookeman, et al., "Lung air spaces: MR imaging evaluation with hyperpolarized 3He gas," *Radiology*, vol. 210, pp. 851–857, 1999.

[35] M. Viallon, Y. Berthèzene, M. Décorps, et al., "Laser-polarized (3)He as probe for dynamic regional measurements of lung perfusion and ventilation using magnetic resonance imaging," *Magnetic Resonance in Medicine*, vol. 44, no. 1, pp. 1–4, 2000.

[36] V. Callot, E. Canet, B. Brochot, et al., "MR perfusion imaging using encapsulated laser-polarized ^{3}He," *Magnetic Resonance in Medicine*, vol. 46, pp. 535–540, 2001.

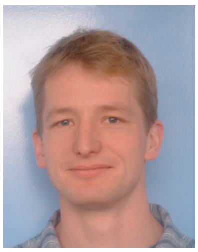

Ralf Lethmate is German born in 1972. He obtained his M.S. degree in 1998 from the University of Cologne, Germany and his Ph.D. degree in magnetic resonance signal processing from the University Claude Bernard Lyon I, France, in 2001. The present work is part of his Ph.D. research. It earned him the Young Investigator Award at ESMRMB Conference in Cannes, France, 22–25 August, 2002. His position was financed by the EU-TMR project CT97-0106. Presently, he is a Product Developer with Soft Imaging System GmbH, Munster, Germany.

Frank Wajer is Dutch born in 1970. He obtained the M.S. and Ph.D. degrees in magnetic resonance signal processing from the Applied Physics Department of the Delft University of Technology (TUD) in 1994 and 2001, respectively. His work was supported by the Dutch Technology Foundation STW and Philips Medical Systems. Presently, he is Radar System Designer at Thales Naval Netherlands.

Yannick Crémillieux is French born in 1965. He obtained his Ph.D. degree in physics in 1994 from the University Claude Bernard Lyon I, France. He is currently a CNRS (Centre National de la Recherche Scientifique) researcher in the CNRS UMR 5012, NMR Laboratory in Lyon, France. His interests are MRI biomedical applications including imaging sequences and methodological developments. His research projects are currently devoted to the biomedical applications of laser-polarized helium3.

Dirk van Ormondt is Dutch born in 1936. He obtained the M.S. and Ph.D. degrees from the Department of Applied Physics, Delft University of Technology (TUD), The Netherlands, in 1959 and 1968, respectively. He was postdoc at the Physics Department, University of Calgary, Calif, USA, with Prof Harvey Buckmaster, during 69/70, and at the Clarendon Laboratory, Oxford, UK, with Dr. Michael Baker, during 70/71. From 1972 till present, he is an Associate Professor at the Department of Applied Physics, TUD. His present research interest is medical magnetic resonance and related signal processing. From 1994 till 2002 he has coordinated European projects on this subject.

Danielle Graveron-Demilly is French born in 1947. She obtained her Chemical Engineering Diploma at INSA-Lyon in 1968, her Ph.D. and Doctorat és Sciences degrees at the University Claude Bernard Lyon I, France, in 1970 and 1984, respectively. In 1968, she joined the Magnetic Resonance Group of the University Claude Bernard Lyon I, as a Research Engineer. She is the Head of Signal Processing team in the CNRS UMR 5012, NMR Laboratory. Her present research interest is methodology and signal processing for medical magnetic resonance imaging and spectroscopy (MRS). She is in charge of the public software package, jMRUI, developed in the context of European projects and designed for medical MRS applications.